

Regional Risk: Supplement

Authors:

C. J. Chamberlain^{1,2}, B. I. Cook³, I. Morales Castilla^{1,4} & E. M. Wolkovich^{1,2}

Author affiliations:

¹Arnold Arboretum of Harvard University, 1300 Centre Street, Boston, Massachusetts, USA;

²Organismic & Evolutionary Biology, Harvard University, 26 Oxford Street, Cambridge, Massachusetts, USA;

³NASA Goddard Institute for Space Studies, New York, New York, USA;

⁴Edificio Ciencias, Campus Universitario 28805 Alcalá de Henares, Madrid, Spain

*Corresponding author: 248.953.0189; cchamberlain@g.harvard.edu

Methods: Spatial predictor

Spatial autocorrelation (SA) is a common issue in spatial ecology given that close spatial units tend to be more similar than units far apart, and thus, cannot be considered as independent units, which is a frequent assumption in statistical tests (Diniz-Filho *et al.*, 2003). If model residuals are spatially autocorrelated, and thus, non-independent then model coefficients and errors may be biased in a hard to predict way (Mauricio Bini *et al.*, 2009). On the contrary, if model residuals are not autocorrelated, then SA should not be of concern (Hawkins, 2012).

To control for spatial autocorrelation and to account for spatially structured processes independent from our regional predictors of false springs, we generate an additional *spatial predictor* for the model. To avoid collinearity, we computed our *spatial predictor* from the residuals of a linear model of false springs as a function of all other regional factors that are also spatially structured (e.g. spring temperature, altitude, distance to the coast), following the logic of spatial filter modelling (Diniz-Filho & Bini, 2005). The calculation of the *spatial predictor* followed the next steps: (a) we fit a linear model of false spring versus regional factors,

$$\begin{aligned}
y_i \sim N(\alpha(i)) &+ \beta_{NAO(i)} + \beta_{MeanSpringTemp(i)} + \beta_{Elevation(i)} + \beta_{DistanceCoast(i)} \\
&+ \beta_{ClimateChange(i)} + \beta_{NAO \times Species(i)} + \beta_{MeanSpringTemp \times Species(i)} + \beta_{Elevation \times Species(i)} \\
&+ \beta_{DistanceCoast \times Species(i)} + \beta_{ClimateChange \times Species(i)} \\
&+ \beta_{NAO \times ClimateChange(i)} + \beta_{MeanSpringTemp \times ClimateChange(i)} + \beta_{Elevation \times ClimateChange(i)} \\
&+ \beta_{DistanceCoast \times ClimateChange(i)} + \sigma_{sp(i)}
\end{aligned}$$

(b) We extracted the residuals of the regression ??, which represent the portion of the variation in the number of false springs that is independent from the predictors in the model. (c) Residuals were utilized as our Y values in a selection of spatial eigenvectors aimed at keeping only the minimal subset of spatial eigenvectors that are able to remove SA from model residuals. Specifically, we selected eigenvectors following the the minimization of Moran's I of the residuals approach (Griffith & Peres-Neto, 2006; Diniz-Filho *et al.*, 2012; David *et al.*, 2017, MIR). (d) We fit a linear model between the residuals of ?? and the subset of selected eigenvectors. And (e) we take the fitted values from this regression as our *spatial predictor* in our final model (see equation from main text), which can be interpreted as a latent variable summarizing the spatial structure in false springs that is unaccounted for by the rest of regional factors in our model (Morales-Castilla *et al.*, 2012). A *spatial predictor* generated in this way has three major advantages. First, it ensures that no SA is left in model residuals. Second, it avoids introducing collinearity issues with other predictors in the model. And third, it can be interpreted as a latent variable summarizing spatial processes (e.g. local adaptation, plasticity, etc.) occurring at multiple scales.

Species rate of budburst calculations

We used data from a growth chamber experiment (Flynn2018) to determine the average number of days between budburst and leafout for our study species. Cuttings for the experiment were made in January 2015 from two field sites: Harvard Forest (HF, 42.5°N, 72.2°W) and the Station de Biologie des Laurentides in St-Hippolyte, Québec (SH, 45.9°N, 74.0°W). The experiment examined budburst and leafout for *Acer saccharum* (Marshall), *Alnus incana* (L.), *Betula papyrifera* (Marshall), *Fagus grandifolia* (Ehrh.), *Fraxinus nigra* (Marshall), and *Quercus alba* (L.) in a fully crossed design of three levels of chilling (field chilling, field chilling plus 30 days at either 1 or 4 °C), two levels of forcing (20°C/10°C or 15°C/5°C day/night temperatures, such that thermoperiodicity followed photoperiod) and two levels of photoperiod (8 versus 12 hour days) resulting in 12 treatment combinations. Phenological observations of each cutting were made every 2-3 days over 82 days. Phenology was assessed using a BBCH scale that was modified for trees (Finn

et al., 2007). We used data from *Acer saccharum* for *Aesculus hippocastanum* (Buerki *et al.*, 2010), *Alnus incana* for *Alnus glutinosa*, *Betula papyrifera* for *Betula pendula* (Wang *et al.*, 2016), *Fagus grandifolia* for *Fagus sylvatica*, *Fraxinus nigra* for *Fraxinus excelsior* and *Quercus alba* for *Quercus robur* (Hipp *et al.*, 2017).

References

- Buerki, S., Lowry II, P., Alvarez, N., Razafimandimbison, S., Kupfer, P. & Callmender, M. (2010) Phylogeny and circumscription of *Sapindaceae* revisited: Molecular sequence data, morphology and biogeography support recognition of a new family, *Xanthoceraceae*. *Plant Ecology and Evolution* **143**, 148–159.
- David, B., Thomas, D., Stéphane, D. & Jason, V. (2017) Disentangling good from bad practices in the selection of spatial or phylogenetic eigenvectors. *Ecography* **0**.
- Diniz-Filho, J.A.F. & Bini, L.M. (2005) Modelling geographical patterns in species richness using eigenvector-based spatial filters. *Global Ecology and Biogeography* **14**, 177–185.
- Diniz-Filho, J.A.F., Bini, L.M. & Hawkins, B.A. (2003) Spatial autocorrelation and red herrings in geographical ecology. *Global ecology and Biogeography* **12**, 53–64.
- Diniz-Filho, J.A.F., Bini, L.M., Rangel, T.F., Morales-Castilla, I., Olalla-Tárraga, M.Á., Rodríguez, M.Á. & Hawkins, B.A. (2012) On the selection of phylogenetic eigenvectors for ecological analyses. *Ecography* **35**, 239–249.
- Finn, G.A., Straszewski, A.E. & Peterson, V. (2007) A general growth stage key for describing trees and woody plants. *Annals of Applied Biology* **151**, 127–131.
- Griffith, D.A. & Peres-Neto, P.R. (2006) Spatial modeling in ecology: the flexibility of eigenfunction spatial analyses. *Ecology* **87**, 2603–2613.
- Hawkins, B.A. (2012) Eight (and a half) deadly sins of spatial analysis. *Journal of Biogeography* **39**, 1–9.
- Hipp, A., S. Manos, P., González-Rodríguez, A., Hahn, M., Kaproth, M., McVay, J., Avalos, S. & Cavender-Bares, J. (2017) Sympatric parallel diversification of major oak clades in the Americas and the origins of Mexican species diversity. *New Phytologist* **217**.
- Mauricio Bini, L., Diniz-Filho, J.A.F., Rangel, T.F., Akre, T.S., Albaladejo, R.G., Albuquerque, F.S., Aparicio, A., Araujo, M.B., Baselga, A., Beck, J. *et al.* (2009) Coefficient shifts in geographical ecology: an empirical evaluation of spatial and non-spatial regression. *Ecography* **32**, 193–204.

Morales-Castilla, I., Olalla-Tarraga, M.A., Purvis, A., Hawkins, B.A. & Rodriguez, M.A. (2012) The imprint of cenozoic migrations and evolutionary history on the biogeographic gradient of body size in new world mammals. *The American Naturalist* **180**, 246–256.

Wang, N., McAllister, H.A., Bartlett, P.R. & Buggs, R.J.A. (2016) Molecular phylogeny and genome size evolution of the genus *Betula* (Betulaceae). *Annals of Botany* **117**, 1023–1035.

Supplement: Tables and Figures

Table 1: Data collected from PEP725 for each species

Species	Num. of Observations	Num. of Sites	Num. of Years
<i>Aesculus hippocastanum</i>	156468	10157	66
<i>Alnus glutinosa</i>	91094	6775	65
<i>Betula pendula</i>	154897	10139	66
<i>Fagus sylvatica</i>	129133	9099	66
<i>Fraxinus excelsior</i>	92665	7327	65
<i>Quercus robur</i>	131635	8811	66

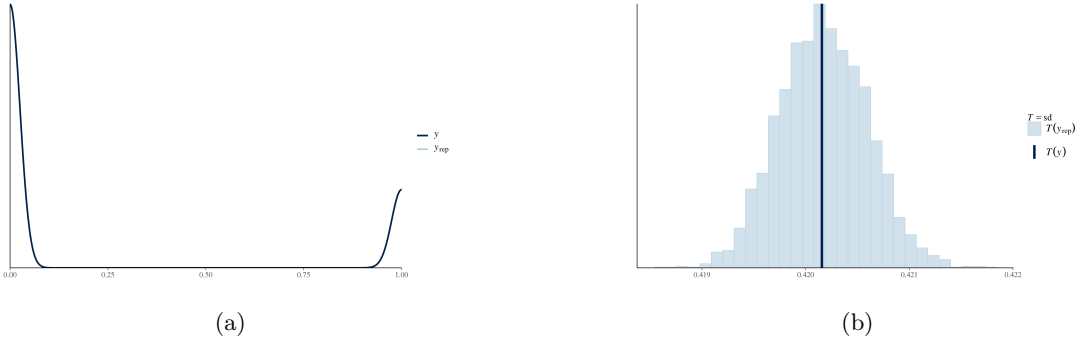


Figure 1: (a) Posterior predictive check comparing the simulated model estimates to the raw data. The curves overlap greatly, which suggests our model is valid and fit the data. (b) Posterior predictive check comparing the standard deviation from our model output to the data. The model fits our data well, which suggests our model is valid.

Table 2: Mean budburst days and confidence intervals for each species for before (1951-1983) and after climate change (1984-2016).

Species (years)	Mean Budburst	2.5%	97.5%
<i>Aesculus hippocastanum</i> (1984-2016)	95.35	95.26	95.44
<i>Alnus glutinosa</i> (1984-2016)	94.90	94.67	95.13
<i>Betula pendula</i> (1984-2016)	95.44	95.23	95.66
<i>Fagus sylvatica</i> (1984-2016)	103.75	103.52	103.97
<i>Fraxinus excelsior</i> (1984-2016)	113.48	113.26	113.71
<i>Quercus robur</i> (1984-2016)	109.60	109.38	109.82
<i>Aesculus hippocastanum</i> (1951-1983)	102.20	102.00	102.41
<i>Alnus glutinosa</i> (1951-1983)	102.81	102.27	103.36
<i>Betula pendula</i> (1951-1983)	101.31	100.81	101.81
<i>Fagus sylvatica</i> (1951-1983)	109.07	108.56	109.59
<i>Fraxinus excelsior</i> (1951-1983)	119.36	118.82	119.89
<i>Quercus robur</i> (1951-1983)	115.85	115.34	116.36

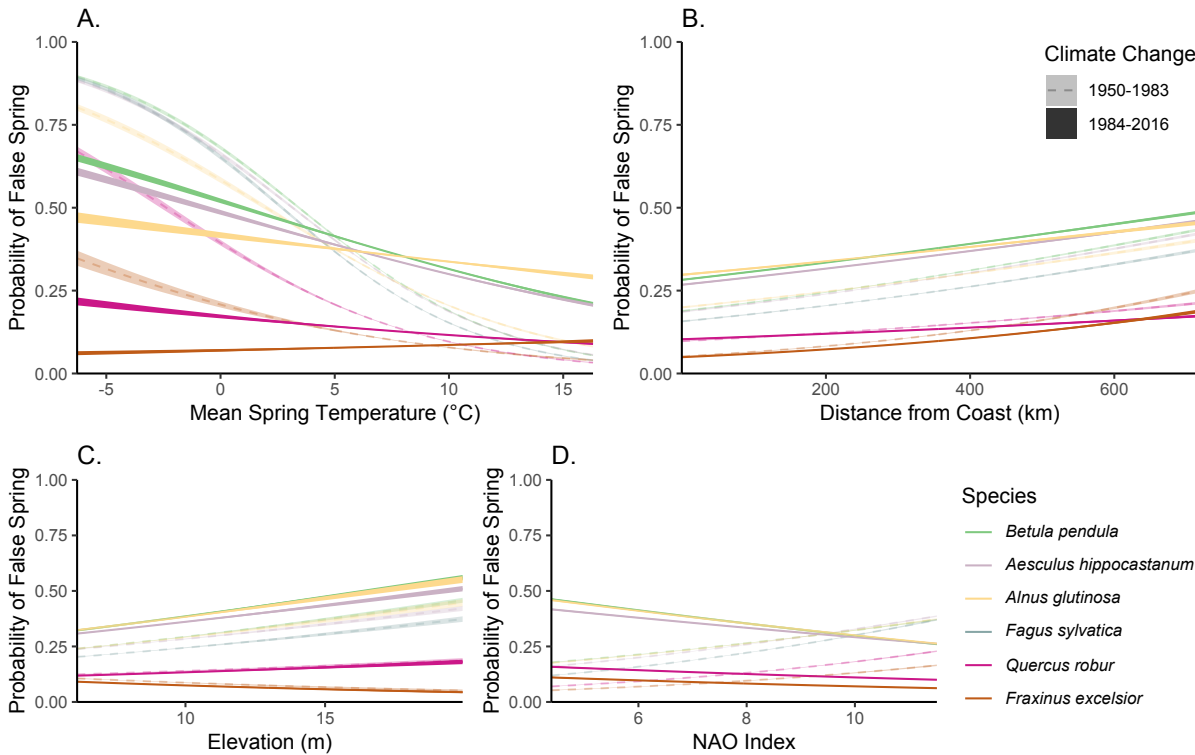


Figure 2: Average predictive comparisons for all climate change interactions with each of the main effects (i.e., mean spring temperature, distance from the coast, elevation, and NAO index). All species are represented.

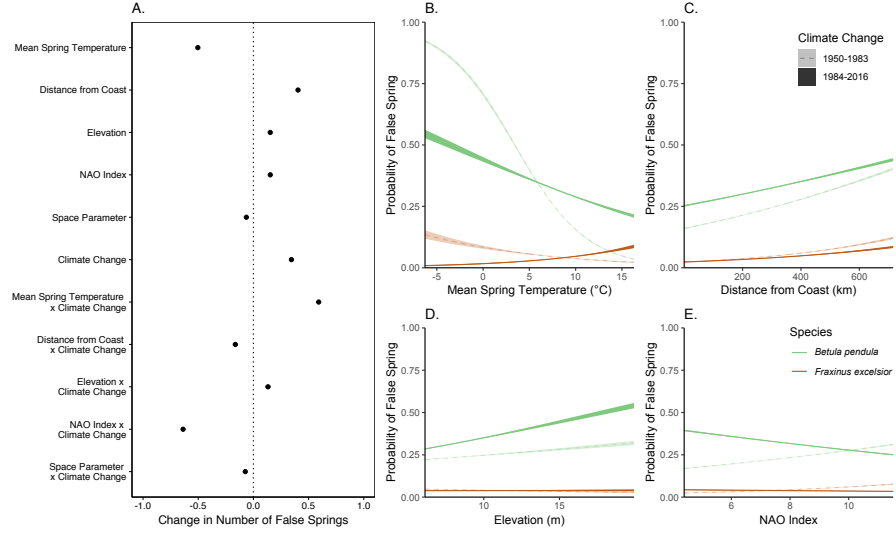


Figure 3: (A) Model output with different durations of vegetative risk for each species. More positive parameter effects indicate an increased probability of a false spring whereas more negative effects suggest a lower probability of a false spring. Uncertainty intervals are at 50%. Parameter effects closer to zero have less of an effect on false springs. There were 622,565 zeros and 132,463 ones for false spring in the data. Panels B-E breakdown the interactions of each of the main effects with climate change (i.e., Mean spring temperature, distance from the coast, elevation, and NAO index). The two extreme species – *Betula pendula* and *Fraxinus excelsior* — were chosen to best represent the variation across all species.

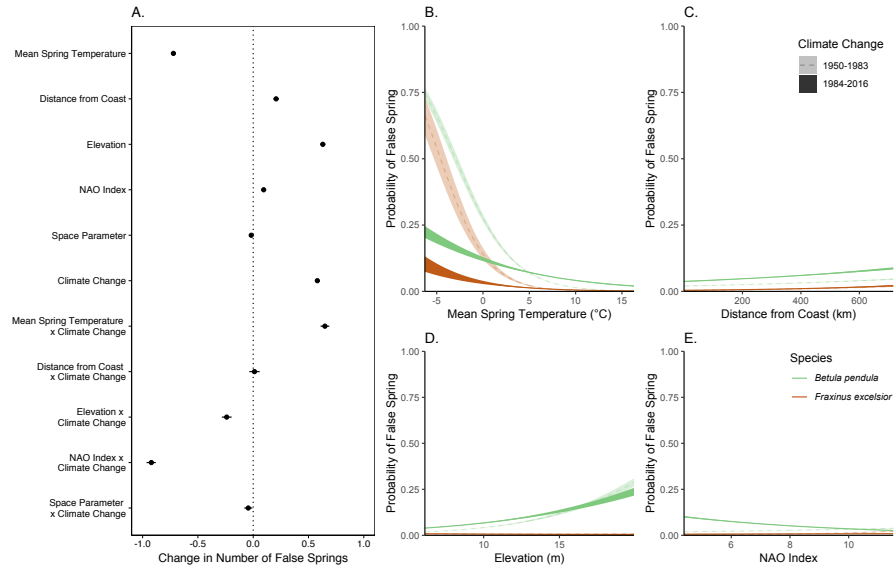


Figure 4: (A) Model output with a lower temperature threshold (-5°C) for defining a false spring. More positive parameter effects indicate an increased probability of a false spring whereas more negative effects suggest a lower probability of a false spring. Uncertainly intervals are at 50%. Parameter effects closer to zero have less of an effect on false springs. There were 730,996 zeros and 23,855 ones for false spring in the data, rendering a less stable model. Panels B-E breakdown the interactions of each of the main effects with climate change.